

Accessing TMDs with semi-inclusive deep-inelastic scattering with CLAS12 at JLab

Stefan Diehl^{a,*} and for the CLAS collaboration

^a*II. Physikalisches Institut, JLU Giessen,
35392, Giessen, Germany*

E-mail: stefan.diehl@exp2.physik.uni-giessen.de

Semi-inclusive deep-inelastic scattering (SIDIS) is a well-established tool to study transverse momentum-dependent parton distribution functions (TMDs) and fragmentation functions. With the CLAS12 detector at Jefferson Laboratory (JLab), precise, multidimensional measurements of cross sections and asymmetry observables become possible in the valence quark regime. The implementation of different unpolarized as well as longitudinally and, in the future, transversely polarized targets in combination with a polarized electron beam provides access to all structure functions of the SIDIS cross section into unpolarized hadrons, while the large acceptance of CLAS12 allows a wide kinematic coverage. Furthermore, different electron beam energies can be used to perform a longitudinal-transverse separation of the SIDIS cross section. This contribution will provide an overview of the ongoing activities in the field of single-hadron and di-hadron SIDIS. A special focus will be set on the extraction of the structure-function ratio $F_{LU}^{\sin\phi}/F_{UU}$ for all three pions and charged kaons over a large range of Q^2 , x_B , z , and P_T .

*7th International Workshop on “Transverse phenomena in hard processes and the transverse structure of the proton (Transversity2024)
3-7 June 2024
Trieste, Italy*

*Speaker

1. Introduction

Transverse momentum dependent parton distribution functions (TMDs) provide a three-dimensional picture of the nucleon by relating the transverse momentum component (k_{\perp}) to the longitudinal momentum fraction (x) of partons (for more details, see e.g. Ref. [1]). In electron scattering experiments like CLAS12 (CEBAF Large Acceptance Spectrometer for experiments at 12 GeV) [2], TMDs can be accessed in semi-inclusive deep-inelastic scattering (SIDIS) processes. The single hadron SIDIS process considers (detects) only one meson besides the scattered lepton, while two mesons are detected in the di-hadron SIDIS process, as shown in Fig. 1. Both processes

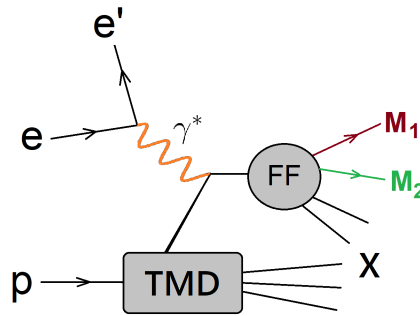


Figure 1: Schematic drawing of the SIDIS process. For the single-hadron SIDIS process, only one meson (M_1) is detected, while the di-hadron SIDIS process requires the detection of two mesons (M_1 and M_2).

are described by a convolution of TMDs and fragmentation functions, which, at the leading twist level, encode the number densities of hadrons produced in the hadronization process of a parton. Single- and di-hadron SIDIS can access the same TMDs but different fragmentation functions.

The CLAS12 spectrometer [2] consists of a forward detector, as well as a central detector and a forward tagger, providing a large acceptance for charged and neutral particles. The forward detector, which is essential for most SIDIS measurements, is designed around a toroidal magnetic field. The magnet coils divide the setup into six identical sectors. In each sector, three regions of drift chambers are used to determine the momentum and the charge of the particles within the magnetic field. The scattered electrons are identified based on a lead-scintillator electromagnetic sampling calorimeter in combination with a Cherenkov counter [2]. Charged hadrons are identified by time-of-flight measurements [3] and by a RICH detector in initially one and later two sectors [4].

1.1 SIDIS Observables with CLAS12 at JLab

The SIDIS process is typically described by the kinematic variables Q^2 , x_B , y , z , P_T , and the angles ϕ between the electron scattering plane and the hadron production plane, as well as the angle ϕ_S between the electron scattering plane and the transverse component of the spin vector of the target nucleon (for a definition of the variables see Ref. [1]). The differential SIDIS cross section

can be expressed in terms of model-independent structure functions by [6, 7].

$$\frac{d\sigma}{dx dy d\phi_s dz d\phi dP_T} \propto \left(F_{UU,T} + \epsilon F_{UU,L} + \sqrt{2\epsilon(1+\epsilon)} \cos\phi F_{UU}^{\cos\phi} + \epsilon \cos 2\phi F_{UU}^{\cos 2\phi} + \lambda_e \sqrt{2\epsilon(1-\epsilon)} \sin\phi F_{LU}^{\sin\phi} \right. \\ + S_L \left[\sqrt{2\epsilon(1+\epsilon)} \sin\phi F_{UL}^{\sin\phi} + \epsilon \sin 2\phi F_{UL}^{\sin 2\phi} \right] + S_L \lambda_e \left[\sqrt{1-\epsilon^2} F_{LL} + \sqrt{2\epsilon(1-\epsilon)} \cos\phi F_{LL}^{\cos\phi} \right] \\ \left. + S_T \left[\sin(\phi - \phi_s) (F_{UT,T}^{\sin(\phi-\phi_s)} + \epsilon F_{UT,L}^{\sin(\phi-\phi_s)}) + \dots \right] + S_T \lambda_e \left[\sqrt{1-\epsilon^2} \cos(\phi - \phi_s) F_{LT}^{\cos(\phi-\phi_s)} + \dots \right] \right), \quad (1)$$

where λ_e is the helicity of the lepton beam and S_L and S_T are the longitudinal and transverse polarization of the target. The variable ϵ represents the ratio of the longitudinal and transverse virtual photon flux. The single structure functions F are related to one or more combinations of a TMD and a fragmentation function. Since the structure functions show intricate kinematic dependencies in the independent kinematic variables x , Q^2 , z and P_T , an isolation of the structure functions from cross-sections and asymmetries, is a challenging task and requires fully differential measurements in terms of the kinematic variables and a knowledge of the full dependence of the cross section on the azimuthal angle ϕ .

CLAS12 is operated in different run groups, depending on the target and the beam energy. The nominal beam energy, used for most run-groups, is typically around 10.6 GeV. The run groups that are relevant for SIDIS studies are listed in Tab. 1. Based on the listed run groups, all structure

run group	target	SIDIS observables
A	un-polarized liq. hydrogen	unpolarized cross sections, F_{LU}
B	un-polarized liq. deuterium	same as RG-A, but u/d flavor separation
C	longitudinally polarized NH ₃ , ND ₃	F_{UL}, F_{LL}
K	un-polarized liq. hydrogen ($E_{beam} = 6.5, 7.5, 8.4$ GeV)	$F_{UU,L} - F_{UU,T}$ separation in combination with RG-A
H	transversely polarized NH ₃	F_{UT}, F_{LT}

Table 1: CLAS12 run groups relevant for SIDIS studies.

functions of the SIDIS cross section can be accessed. While run groups A, B, C, and K have already taken at least a part of the approved statistics and will complete the data taking in the following years, run group H is currently scheduled to take data in 2029 [5].

2. Single Hadron SIDIS

2.1 Beam Spin Asymmetries

As a first published observable, the structure function ratio $F_{LU}^{\sin\phi}/F_{UU}$ has been extracted based on beam spin asymmetry measurements. The denominator F_{UU} is in leading order only related to a convolution of the well known unpolarized TMD f_1 and the unpolarized fragmentation function D_1 , while the structure function $F_{LU}^{\sin\phi}$ can be related to a convolution (ζ) of TMDs (green)

and fragmentation functions (blue) [8]:

$$F_{LU}^{\sin\phi} = \frac{2M}{Q} \zeta \left(-\frac{\hat{\mathbf{h}} \cdot \mathbf{k}_T}{M_h} \left(x e H_1^\perp + \frac{M_h}{M} f_1 \frac{\tilde{G}^\perp}{z} \right) + \frac{\hat{\mathbf{h}} \cdot \mathbf{p}_T}{M} \left(x g^\perp D_1 + \frac{M_h}{M} h_1^\perp \frac{\tilde{E}}{z} \right) \right). \quad (2)$$

It is expected that the eH_1^\perp term, which convolutes the twist-3 TMD e and the Collins FF H_1^\perp and the $g^\perp D_1$ term, including the twist-3 T-odd distribution function g^\perp and the unpolarized FF D_1 , provide the dominant contributions. The other terms with the twist-3 FF \tilde{G}^\perp and \tilde{E} and the unpolarized distribution function f_1 and the Boer-Mulders function h_1^\perp (both twist-2), provide additional minor contributions. However, the relative contributions depend on the kinematic region and need to be validated based on detailed, fully differential measurement of $F_{LU}^{\sin\phi}$ and other SIDIS structure functions.

The first results of a fully differential, high precision study of $F_{LU}^{\sin\phi}/F_{UU}$ for single π^+ SIDIS have been published in Ref. [9] in comparison to TMD-based predictions based on the models described in Ref. [10, 11]. The study has been extended to the other pion flavors with the same kinematic binning. Preliminary results for all three pion flavors are shown in Fig. 2 for selected z bins and for four of the nine $Q^2 - x_B$ bis shown in the right part of the figure. It can be observed

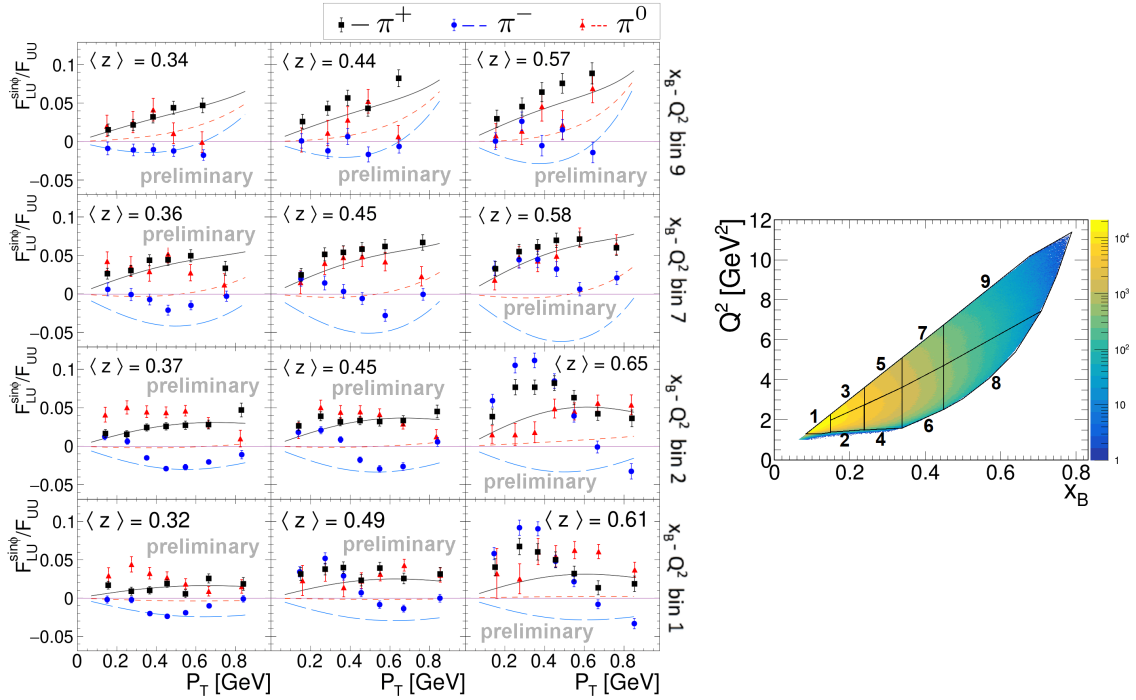


Figure 2: Preliminary results for the structure function ratio $F_{LU}^{\sin\phi}/F_{UU}$ as a function of P_T for selected multidimensional bins of z , Q^2 , and x_B for π^+ (black), π^- (blue), and π^0 (red) [12]. The solid and dashed lines show TMD-based predictions based on the models in Refs. [10, 11] with the color corresponding to the meson.

that the structure function ratios for π^+ and π^0 are both positive and show similar magnitudes in some kinematic regions. If $F_{LU}^{\sin\phi}$ would be dominated by the Collins term ($e H_1^\perp$) of $F_{LU}^{\sin\phi}$ only, a clear hierarchy $F_{LU}^{\sin\phi}(\pi^-) < F_{LU}^{\sin\phi}(\pi^0) = 0 < F_{LU}^{\sin\phi}(\pi^+)$ would be expected. This behavior

is not reflected by the data and the current theoretical models. The observed behavior indicates a significant contribution of additional terms, like the $g^\perp D_1$ term, for which current theoretical models [10, 11] show a more dominant role at larger Q^2-x_B values. The high precision, fully differential data from CLAS12 will help to constrain these TMD-based models. However, it can be clearly observed that the "bumping" structures, which show up especially at low P_T and high z in the low Q^2-x_B region, cannot be reproduced by the TMD-based models. Studies showed that these structures at least partly originate from exclusive ρ meson production ($ep \rightarrow e'p'\rho^0$), which is consistent with their absence in the case of π^0 SIDIS. Further studies on this exclusive ρ^0 contribution are ongoing and will be published soon.

Besides single-pion SIDIS, also single-kaon SIDIS has been studied [13]. For this study the Kaons were identified by a neural network, using the time of flight information as well as different other detector information, like the energy deposition in the calorimeter, as an input. The remaining pion information was identified and subtracted to obtain the pure kaon results. These studies are important to identify the contribution of strange-quark TMDs and of differences in the fragmentation functions for pion and kaon production. Figure 3 shows preliminary results for $F_{LU}^{\sin\phi}/F_{UU}$ of K^+ SIDIS in comparison to the π^+ results and to TMD-based theory predictions for selected z bins and for the three Q^2-x_B bins shown in the right part of the figure. It can be observed that the $F_{LU}^{\sin\phi}/F_{UU}$

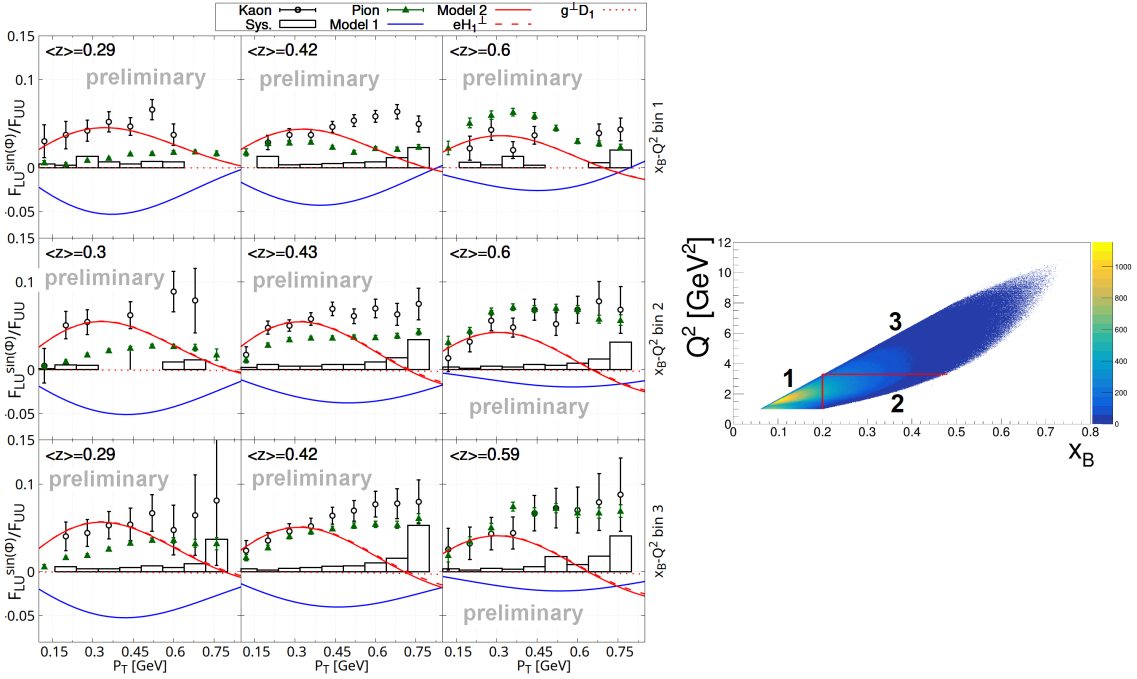


Figure 3: Preliminary results for $F_{LU}^{\sin\phi}/F_{UU}$ of K^+ SIDIS (open circles) in comparison to π^+ SIDIS (green triangles) as a function of P_T for selected multidimensional bins of z , Q^2 , and x_B [13]. The white histogram shows the systematic uncertainty of the K^+ study, and the lines show the predictions from the two TMD-based models described in Refs. [10, 11].

values for K^+ and π^+ are both positive. At small z , K^+ shows a larger magnitude than π^+ while the results get more similar at higher z values. The precise measurement allows a direct judgment between the two theory models. While the first model (blue) clearly describes a different trend than

the data, a good agreement between data and theory can be observed for the second model (red).

2.2 Multiplicities and unpolarized moments

Besides the shown studies of the structure function ratio $F_{LU}^{\sin\phi}/F_{UU}$, further studies are ongoing for the un-polarized multiplicities and the $\cos\phi$ and $\cos 2\phi$ moments of the un-polarized single hadron SIDIS cross section. The multiplicity is defined as:

$$\frac{d^2 M^h(x_B, Q^2, z, P_T^2)}{dz dP_T^2} = \frac{d^4 \sigma^{SIDIS}}{dx_B dQ^2 dz dP_T^2} / \frac{d^2 \sigma^{DIS}}{dx_B dQ^2}, \quad (3)$$

with the SIDIS cross section (σ^{SIDIS}) and the cross section from deeply-virtual inclusive electron scattering (σ^{DIS}). Since multiplicities are typically integrated over ϕ , they mainly show a sensitivity to $F_{UU,T} = \zeta[f_1 D_1]$ in leading order [8]. Currently, different studies of multiplicities, especially for single π^0 SIDIS [14], are in progress based on CLAS12 data.

The $\cos\phi$ and $\cos 2\phi$ moments show the following leading twist connection to TMDs [8]:

$$F_{UU}^{\cos\phi} = \frac{2M}{Q} \zeta \left(-\frac{\hat{\mathbf{h}} \cdot \mathbf{k}_T}{M_h} \left(x h H_1^+ + \frac{M_h}{M} f_1 \frac{\tilde{D}^\perp}{z} \right) + \frac{\hat{\mathbf{h}} \cdot \mathbf{p}_T}{M} \left(x f^\perp D_1 + \frac{M_h}{M} h_1^\perp \frac{\tilde{H}}{z} \right) \right), \quad (4)$$

$$F_{UU}^{\cos 2\phi} = \zeta \left[-\frac{2(\hat{\mathbf{h}} \cdot \mathbf{k}_T)(\hat{\mathbf{h}} \cdot \mathbf{p}_T) - \mathbf{k}_T \cdot \mathbf{p}_T}{M M_h} h_1^\perp H_1^+ \right], \quad (5)$$

However, potential next to leading twist contributions are expected to show a sensitivity to the Cahn effect. At the moment, advanced differential (Q^2 , y , z , and P_T) measurements of both moments are ongoing for pion [15] and kaon SIDIS data of CLAS12 and will help to identify these next-to-leading-order effects and their kinematic dependence.

3. Di-Hadron SIDIS

Di-hadron SIDIS, with the detection of two final state mesons, can provide additional constraints for TMDs by introducing additional observables and therefore degrees of freedom. Here, on the one side, the sum of the two hadrons \vec{P}_h , but also the relative momentum \vec{R} of the hadron pair:

$$\vec{P}_h = \vec{P}_1 + \vec{P}_2 \quad \vec{R} = \frac{1}{2}(\vec{P}_1 - \vec{P}_2), \quad (6)$$

contain information about the correlations in the final state. The planes spanned by the two vectors lead to two azimuthal angles ϕ_h and ϕ_R , relative to the electron scattering plane.

As an example, the moment $A_{LU}^{\sin\phi_R}$ is related to the twist-3 TMD $e(x)$. Furthermore, di-hadron SIDS allows the study of DiFFs with no single hadron analog, like G_1^\perp , which describes the azimuthal dependence of an unpolarized hadron pair on the helicity of the outgoing quark and is related to the $A_{LU}^{\sin(\phi_h - \phi_R)}$ moment of the di-hadron SIDIS process. Details on the di-hadron cross-section and the involved structure functions can be found e.g. in Ref. [16].

As a first process, $ep \rightarrow e'\pi^+\pi^-X$ was studied with CLAS12, and the $A_{LU}^{\sin\phi_R}$ moment as a function of x as well as the $A_{LU}^{\sin(\phi_h - \phi_R)}$ moment as a function of the di-hadron mass were extracted in Ref. [17]. Based on this data, a first extraction of $e(x)$ became possible [18]. Further studies

of the $e'\pi^+\pi^-X$ final state based on proton and deuterium targets are currently ongoing [19] with the goal to perform a flavor decomposition of the involved twist-3 PDFs. In addition, the study of the $e\pi^\pm\pi^0$ final states [20] and the inclusion of charged Kaons in the di-hadron sample [21], will provide additional important insights into the role of the different contributions to the measured moments.

A special case of di-hadron SIDIS is given by Λ SIDIS, with the Λ reconstructed from a proton and a π^- in the inclusive final state. Here, the self-analyzing decay of the Λ can be used to determine the longitudinal spin transfer $D_{LL'}$ from a polarized electron beam scattering off an unpolarized proton target to the hyperon. Based on this quantity, the helicity dependent fragmentation function G_1^Λ , which provides insight into the spin structure of the Λ , can be accessed in addition to $e(x)$ if the Λ s are produced in the current fragmentation region [22]. The new CLAS12 data will help to better constrain the existing models on the spin structure of the Λ . More details and first results can be found in Ref. [23].

4. Longitudinally and transversely polarized targets

Recently, the first data-taking period with a longitudinally polarized ammonia (NH_3) target was completed [24]. The target shows a dilution factor of $\sim 3/17$ and a polarization of $\sim 85\%$. Based on this newly recorded data, a rich physics program for the longitudinally polarized SIDIS structure functions in single and di-hadron SIDIS is currently under way. First results can be found in Ref. [25]

As a last missing step to access also the transversely polarized structure functions, a "conventional" transversely polarized NH_3 target is under preparation, and data taking is currently planned for 2029. The characteristics of this target will be very similar to the longitudinally polarized target, with an expected dilution factor of $\sim 3/17$ and a polarization of $\sim 85\%$ [26]. Due to the transverse holding field, the luminosity of CLAS12 will be limited by the Moeller scattering. A conservative estimate assumes that $\sim 1/50$ of the „regular“ CLAS12 luminosity can be reached. Nevertheless, the expected data will not only increase the kinematic region but also significantly advance the statistics of the existing lepton scattering data with transversely polarized targets.

5. Summary and Outlook

In summary, CLAS12 provides several orders of magnitude higher luminosity than any previous lepton scattering experiment. High precision data in the valence region for unpolarized proton and deuteron targets and for a longitudinally polarized target have already been recorded. Based on this data, CLAS12 allows high precision multidimensional studies, studies of different polarization observables, studies of flavor dependencies, as well as analyses beyond the leading twist left and the current fragmentation regime. First longitudinal beam asymmetries have been published, and more results for the unpolarized proton target and results for a longitudinally polarized target, as well as results for a neutron target (deuteron), will follow. A run with a transversely polarized target is scheduled for 2029.

Acknowledgements

S. Diehl is supported by Deutsche Forschungsgemeinschaft (Project No. 508107918).

References

- [1] S. Diehl, "Experimental Exploration of the 3D Nucleon Structure", *Progress in Particle and Nuclear Physics*, 104069 (2023). doi:10.1016/j.pnpnp.2023.104069
- [2] V. D. Burkert et al. (CLAS Collaboration), *NIM A* **959**, 163419 (2020). doi:10.1016/j.nima.2020.163419
- [3] D. S. Carman, L. Clark, R. De Vita, et al., *Nucl. Inst. and Meth. A* 960, 163629 (2020). doi:10.1016/j.nima.2020.163629
- [4] M. Mirazita, G. Angelini, I. Balossino, et al., *Nucl. Inst. and Meth. A* 952, 161844 (2020). doi:10.1016/j.nima.2019.01.070
- [5] D. Higinbotham, Jefferson Lab's 12GeV Experimental Schedule, talk at the CLAS CM March 2024, <https://indico.jlab.org/event/829/contributions/14068/attachments/10719/16238/Higinbotham%20-%20Experimental%20Schedule%20and%20Future%20Directions.pptx>
- [6] P. J. Mulders, R. D. Tangerman, *Nucl. Phys. B* **461**, 197 (1996). doi:10.1016/0550-3213(95)02900632-X
- [7] A. Bacchetta, M. Diehl, K. Goeke, et al., *J. High Energ. Phys.* **02**, 093 (2007). doi:10.1088/1126-6708/2007/02/093
- [8] A. Bacchetta, M. Diehl, K. Goeke, A. Metz, P. J. Mulders and M. Schlegel, *J. High Energ. Phys.* **02**, 093 (2007). doi:10.1088/1126-6708/2007/02/093
- [9] S. Diehl et al. (CLAS Collaboration), *Phys. Rev. Lett.* **128**, 062005 (2022). doi:10.1103/PhysRevLett.128.062005
- [10] W. Mao and Z. Lu, *Eur. Phys. J. C* **73**, 2557 (2013). doi:10.1140/epjc/s10052-013-2557-9
- [11] W. Mao and Z. Lu, *Eur. Phys. J. C* **74**, 2910 (2014). doi:10.1140/epjc/s10052-014-2910-7
- [12] S. Diehl et al. (CLAS collaboration), to be published.
- [13] A. Kripko, S. Diehl et al. (CLAS collaboration), to be published, presented e.g. at the workshop on Present and future perspectives in Hadron Physics, Frascati (2024) https://agenda.infn.it/login/?next=/event/38467/contributions/234436/attachments/122303/178823/Kaon_Kripko_workshop2024.pdf
- [14] M. Scott, *Proceedings of Science 456 (Spin 2023)* (2024). doi: 10.22323/1.456.0068

- [15] R. Capobianco, talk at the International workshop on CLAS12 physics and future perspectives at JLab, Paris (2023) <https://indico.jlab.org/event/9131/contributions/28970/> and at the 2023 Fall Meeting of APS DNP and JPS (2023).
- [16] S. Gliske, A. Bacchetta and M. Radici, Phys. Rev. D 90, 114027 (2014). [Erratum: Phys. Rev. D 91, 019902 (2015)]. doi:10.1103/PhysRevD.91.019902
- [17] T. Hayward et al. (CLAS), Phys. Rev. Lett. **126**, 152501 (2021). doi:10.1103/PhysRevLett.126.152501
- [18] A. Courtoy et al., Phys. Rev. D **106**, 014027 (2022). doi:10.1103/PhysRevD.106.014027
- [19] C. Dilks, talk at Transversity 2022 (Pavia, Italy). <https://agenda.infn.it/event/19219/contributions/170922/attachments/91270/123838/dilks-dihadrons-transversity2022.pdf>
- [20] G. Matousek and A. Vossen, JINST 19 C06006 (2024). doi: 10.1088/1748-0221/19/06/C06006
- [21] C. Pecar, talk at the workshop on Kaons at CLAS12 (Frascati, Italy, 2022) https://agenda.infn.it/event/33338/contributions/186907/attachments/100398/139686/ALU_frascati_2022_final.pdf
- [22] A. Airapetian et al., Phys. Rev. D 74, 072004 (2006). doi:10.1103/PhysRevD.74.072004
- [23] M. McEneaney, JPS Conf. Proc., 020304 (2022). doi:10.7566/JPSCP.37.020304
- [24] C. Keith, J. Brock, C. Carlin, T. Kageya, V. Lagerquist, J. Maxwell and P. Pandey, Proceedings of Science 433 (PSTP2022), (2023). doi:10.22323/1.433.0009
- [25] H. Avakian, talk "TMD program at JLab" at SPIN2023, <https://indico.jlab.org/event/663/contributions/13420/>
- [26] Proposal to PAC39: "Target Single Spin Asymmetry in Semi-Inclusive Deep-Inelastic (e, e', π^\pm) Reaction on a Transversely Polarized Proton Target", available at https://www.jlab.org/exp_prog/proposals/12/C12-11-108.pdf